Bioorganic & Medicinal Chemistry Letters 20 (2010) 7414–7420

Contents lists available at ScienceDirect

Bioorganic & Medicinal Chemistry Letters

journal homepage: www.elsevier.com/locate/bmcl

Discovery of novel quinolinone adenosine A_{2B} antagonists

Brian F. McGuinness [a,*], Koc-Kan Ho [a], Tara M. Stauffer [a], Laura L. Rokosz [a], Neelima Mannava [a], Steven G. Kultgen [a], Kurt Saionz [a], Anthony Klon [a], Weiqing Chen [a], Hema Desai [a], W. Lynn Rogers [a], Maria Webb [a], Juxing Yin [b], Yan Jiang [b], Tailong Li [b], Hao Yan [b], Konghua Jing [b], Shengting Zhang [b], Kanak Kanti Majumdar [c], Vikash Srivastava [c], Samiran Saha [c]

[a] Ligand Pharmaceuticals, 3000 Eastpark Boulevard Cranbury, NJ 08512, USA
[b] WuXi AppTec Co., Ltd, 288 Fute Zhong Road, Shanghai 200131, China
[c] TCG Lifesciences Ltd (Chembiotek), Block BN, Plot-7, Sec-V, Salt Lake City, Kolkata 700 091, India

ARTICLE INFO

Article history:
Received 4 September 2010
Revised 5 October 2010
Accepted 6 October 2010
Available online 4 November 2010

Keywords:
A_{2B} receptor
Adenosine
Antagonist
Combinatorial chemistry
Quinolinone

ABSTRACT

A novel series of quinolinone-based adenosine A_{2B} receptor antagonists was identified via high throughput screening of an encoded combinatorial compound collection. Synthesis and assay of a series of analogs highlighted essential structural features of the initial hit. Optimization resulted in an A_{2B} antagonist (**2i**) which exhibited potent activity in a cAMP accumulation assay (5.1 nM) and an IL-8 release assay (0.4 nM).

Extracellular adenosine provides regulatory signals through interaction with a family of G-protein coupled adenosine receptors (subtypes A_1, A_{2A}, A_{2B}, and A_3).[1] In lung tissue, for example, interaction of extracellular adenosine with the A_{2B} receptor has been shown to cause the release of pro-inflammatory cytokines.[2] Hence, antagonism of the A_{2B} adenosine receptor subtype has been proposed as a treatment for respiratory disease.[3] A_{2B} antagonists have also been suggested as treatments for diabetes,[4] diabetic retinopathy,[5] colitis,[6] and cancer.[7] Efforts to develop selective, small molecule A_{2B} antagonists have originally stemmed from xanthine-based lead structures such as MRS-1754.[8] Optimization of this lead led to CVT-6883, a selective A_{2B} antagonist which entered human clinical trials.[9] Non-xanthine-based A_{2B} antagonists have also been discovered including 2-aminopyrimidines,[10] *N*-(5,6-diarylpyridin-2-yl) amides,[11] 2-aminobenzothiazoles,[12] and aminothiazoles.[13]

We have previously described the discovery of various A_{2A} receptor antagonists via the high throughput screening of a large, encoded combinatorial compound collection.[14–16] Herein, we detail the optimization of a novel series of A_{2B} antagonists based on quinolinone hits also discovered from this encoded combinatorial collection.[17]

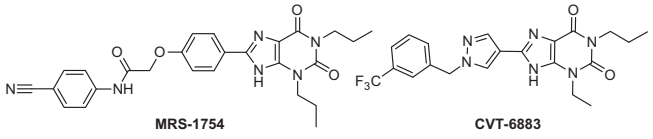

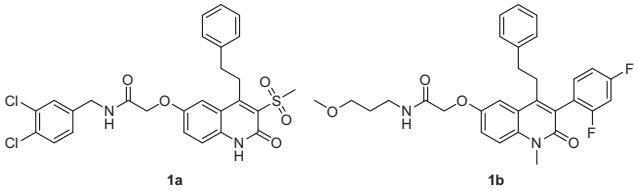

Two hit molecules, **1a** and **1b**, were initially identified as A_{2B} antagonists. While both were active in a hA_{2B} cAMP accumulation assay (Table 1), neither was stable in a human liver microsome assay (0% remaining after 0.5 h treatment with human liver microsomes).[18] In addition, while these hits proved highly selective against the A_{2A} receptor subtype, they exhibited only minimal A_1 receptor selectivity. Hence, a series of analogs aimed at increasing both human liver microsome (HLM) stability and A_1 receptor selectivity were synthesized.

* Corresponding author. Tel.: +1 609 570 1095 x1527; fax: +1 609 570 1050.
E-mail address: bmcguinness@venenumbiodesign.com (B.F. McGuinness).

0960-894X/$ - see front matter © 2010 Elsevier Ltd. All rights reserved.
doi:10.1016/j.bmcl.2010.10.030

Table 1
SAR of quinolinone analogs

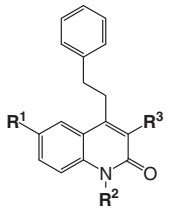

Compd	R^1	R^2	R^3	CHO-hA_{2B} cAMP K_i (nM)	Human A_{2B} binding av K_i (nM)	Human A_{2A} binding av K_i (nM)	A1 binding av K_i (nM)	HLM stability (% remaining-0.5 h)[13]
1a	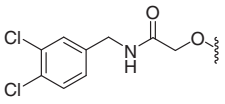	H		315 ± 102	211 ± 36	>10,000	811 ± 6	0
1b	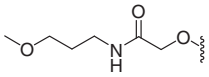	Me	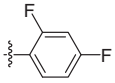	633 ± 83	677 ± 44	>10,000	3623 ± 1536	0
1c	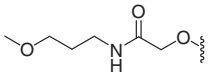	H	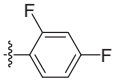	>5000	>10,000	>10,000	6050 ± 3175	ND
1d	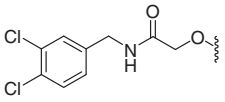	Me		>5000	>7000	ND	>10,000	ND
1e	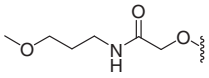	H		>5000	ND	>10,000	10,443 ± 5032	ND
1f	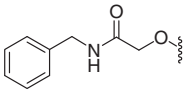	H		352 ± 227	70 ± 19	>10,000	159 ± 34	0
1g	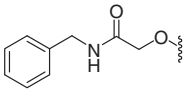	Me	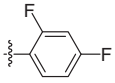	>5000	3655 ± 1332	>10,000	7027 ± 616	ND
1h		H		3474 ± 739	11,310 ± 470	>10,000	>10,000	28
1i	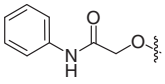	H		1675 ± 671	>10,000	>10,000	1334 ± 309	67
1j	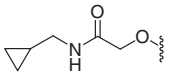	H		>5000	>10,000	ND	>10,000	ND
1k	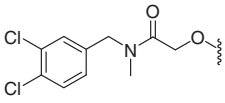	H		1017 ± 37	710 ± 44	>10,000	602 ± 25	0

The synthetic route used to generate the majority of the analogs in this study is outlined in Scheme 1. The hydroxyl moiety of 4-aminophenol was protected as the *t*-butyldimethylsilyl ether followed by protection of the amino group as the *t*-butoxycarbamate. The dianion of this protected intermediate was reacted with tributyltin chloride to generate stannane **4** which was employed in a Stille coupling with the appropriate acid chloride to yield ketone **5**. Deprotection of the phenol and alkylation with methyl bromoacetate produced **6** which was further deprotected by TFA treatment to yield aniline **7**.

Various methods were employed at this stage to generate the quinolinone ring (**8**) depending on the targeted R^3 group. For the methanesulfonyl and 2,4-difluorophenyl R^3 analogs, a two step procedure of amide formation followed by base-mediated cyclization was required. For the 2-thiazolyl R^3 analogs, however, cyclization occurred spontaneously with warming during the EDC-mediated amide formation conditions. The required 2-thiazolylacetic acid was prepared by the homologation route described in Scheme 2. Although phosphorus oxychloride (employed for the synthesis of analogs **2n**–**2q**) was also effective in producing a cyclized structure, the 2-chloroquinoline was isolated. Subsequent treatment with acetic acid under microwave heating was employed to produce the desired quinolinone **8**.

If desired, methylation of the R^2 position was completed at this stage (**8**) via methyl iodide treatment in the presence of potassium carbonate. Ultimately, base-mediated deprotection of the methyl ester followed by amide bond formation yielded the completed analogs.

A similar route was followed to generate the aminomethyl quinolinones **2d**–**2f** (Scheme 3). 4-Chloroaniline was Boc-protected and

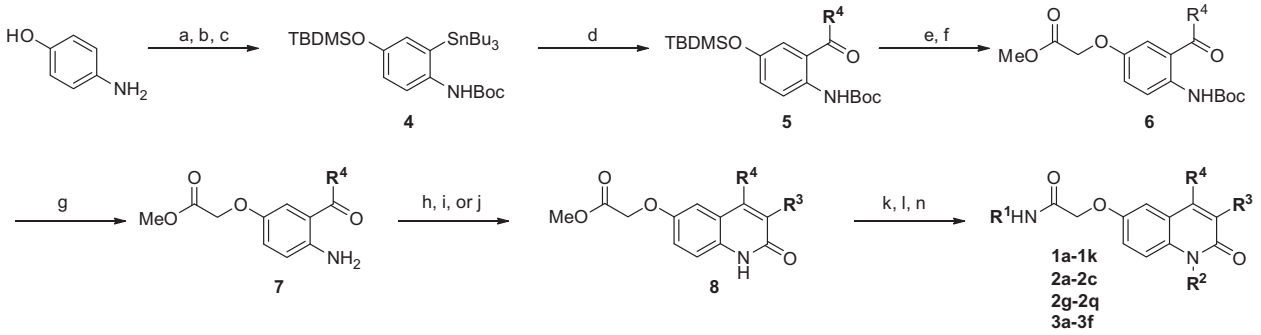

Scheme 1. Synthetic route for quinolinone-6-oxyacetamide analogs. Reagents and conditions: (a) TBDMSCl, imidazole, THF, rt; (b) Boc anhydride, DCM, rt; (c) *n*-BuLi (1 equiv), *t*-BuLi (1 equiv), $(Bu)_3SnCl$, THF, −78 °C; (d) R^4COCl, $[Pd(CH_3CN)_2]Cl_2$, toluene, 100 °C; (e) TBAF, THF, rt; (f) methyl bromoacetate, K_2CO_3, MeCN, rt; (g) TFA; DCM, rt; (h) for $\mathbf{R^3}$ = methanesulfonyl and 2,4-difluorobenzyl: (i) $\mathbf{R^3}CH_2COOH$, EDC, HOBt, DIEA, DMF, rt; (ii) NaOMe, MeOH, 65 °C; (i) for $\mathbf{R^3}$ = thiazolyl: 2-(thiazol-2-yl)acetic acid (**13**), EDC, HOBt, DMF, 55 °C; (j) For analogs **2n**–**2q**: (i) $\mathbf{R^3}CH_2COOH$, $POCl_3$ 50 °C; (ii) acetic acid, mw, 140 °C, 80 min; (k) (only for analogs **1b**, **1d**, and **1e**) MeI, K_2CO_3, MeCN, rt; (l) LiOH, THF, H_2O, rt; (n) $\mathbf{R^1}NH_2$, EDC, HOBt, DIEA, THF, rt.

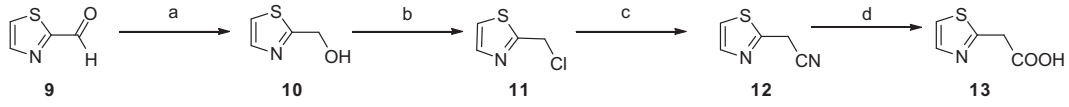

Scheme 2. Synthesis of 2-(thiazol-2-yl)acetic acid (**13**). Reagents and conditions: (a) $NaBH_4$, MeOH, rt; (b) Ph_3P, CCl_4, 60 °C; (c) TMSCN, TBAF, DCM, rt; (d) 9% aq KOH, 100 °C.

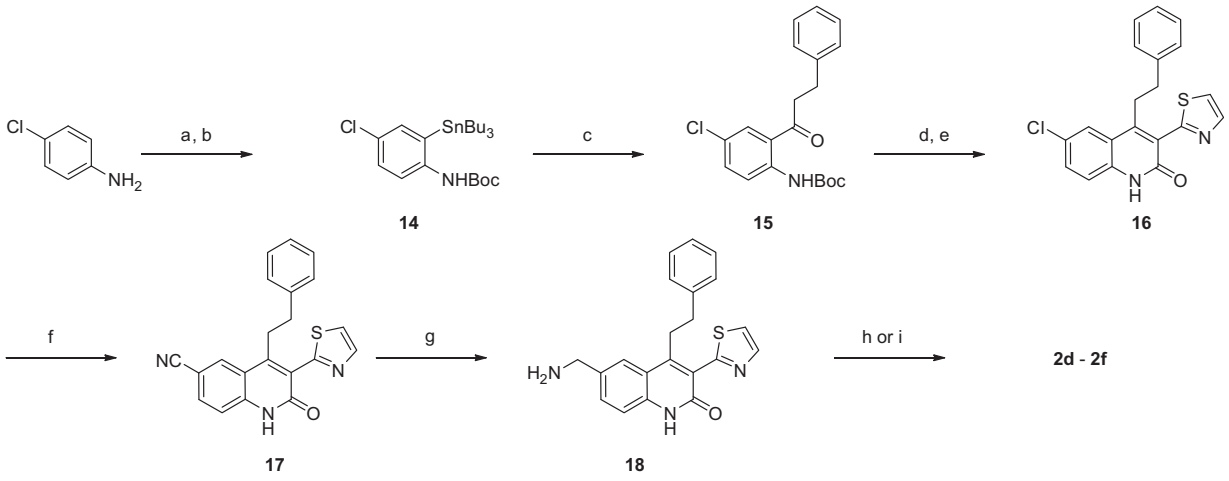

Scheme 3. Synthesis route for analogs **2d**–**2f**. Reagents and conditions: (a) Boc anhydride, THF, rt; (b) *n*-BuLi (1 equiv) *t*-BuLi (1 equiv), $(Bu)_3SnCl$, THF, −78 °C; (c) hydrocinnamoyl chloride, $[Pd(CH_3CN)_2]Cl_2$, toluene, 100 °C; (d) TFA; DCM, rt; (e) 2-(thiazol-2-yl)acetic acid, EDC, HOBt, DMF, 55 °C; (f) $Zn(CN)_2$, $Pd(TFA)_2$, (binaphthyl)P(*t*-$Bu)_2$, DMA, mw, 180 °C 1 h; (g) H_2, Raney Ni, THF, NH_3, MeOH, H_2O, rt; (h) for analog **2d**: hydrocinnamoyl chloride, Et_3N, DCM, rt; (i) benzylamine (for **2e**) or cumylamine (for **2f**), triphosgene, DIEA, DCM, rt.

converted to the tributyltin derivative (**14**) as outlined above. Stille coupling with hydrocinnamoyl chloride produced intermediate **15** which could be cyclized to the quinolinone (**16**) as before. Palladium-mediated conversion to the cyanoquinolinone (**17**) followed by reduction with Raney nickel generated the aminomethyl derivative **18** which could be converted to the desired urea or amide derivatives by standard protocols.

The synthesized analogs[19] were tested for A_{2B} receptor activity in a CHO-based cAMP accumulation assay,[20] an A_{2B} binding assay,[21] and ultimately a HMC-1 cell IL-8 release assay.[22] Compounds were also tested in A_{2A} and A_1 binding assays to access subtype selectivity.[23]

A divergent SAR pattern was observed between analogs of the two initial hit structures **1a** and **1b** (Table 1). Analog **1c** (the R^2-desmethyl analog of 2,4-difluorophenyl-containing **1b)** was not active in the A_{2B} cAMP assay. Additionally, analog **1d** (the N-1 methyl derivative of methylsulfone-containing **1a)** lacked potency. Pairing of the 3-methoxypropylamide R^1 tail of **1a** with the 3-(methylsulfonyl)-quinolinone scaffold of analog **1b** also led to inactivity (**1e**). Finally, while the presence of a simplified R^1 benzylamine was allowed on the 3-(methylsulfonyl)-quinolinone scaffold (**1f**), matching of the R^1 benzylamine with the 3-(2,4-difluorophenyl)quinolinone scaffold was not tolerated (**1g**). Hence, analogs of **1a** and **1b** exhibited distinct SAR. Because the *c* log *P* of analog **1f** (2.0) was significantly lower than that of analog **1b** (4.9), efforts were focused on optimizing the 3-methylsulfone series.[24]

The presence of an oxyacetamide in the initial hit structures **1a** and **1b** was reminiscent of the 8-phenyl xanthine analog MRS-1754. It was clear that this portion of the molecule was important since the truncated methoxy analog **1h** was only weakly active. However, the *N*-phenyloxyacetamide analog **1i** exhibited a loss in potency, indicating the quinolinone series did not follow the

Table 2
SAR of quinolinone analogs

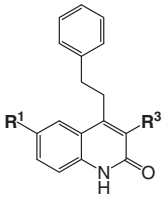

2a	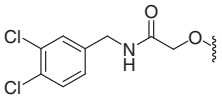		667 ± 47	338 ± 187	408 ± 171	>10,000	1085 ± 516	0
2b	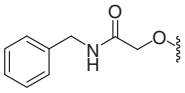		330 ± 29	1124 ± 440	407 ± 190	>10,000	436 ± 105	0
2c	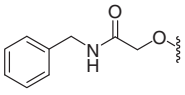		21 ± 3	37 ± 9.5	61 ± 18	3509 ± 83	101 ± 57	2
2d	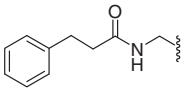		1926 ± 1621	291 ± 74	ND	>10,000	3253 ± 752	3
2e	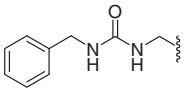		68 ± 29	19 ± 4.3	ND	>10,000	68 ± 2	4
2f	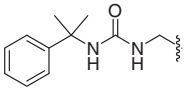		17 ± 3.3	ND	ND	>10,000	68 ± 37	40
2g	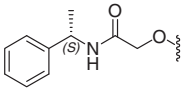		15 ± 8	28 ± 0.7	1.7 ± 0.4	2439 ± 184	15 ± 12	3
2h	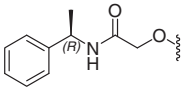		320 ± 44	486 ± 113	60 ± 32	>10,000	170 ± 70	ND
2i	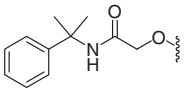		5.1 ± 1.1	28 ± 8.4	1.3 ± 0	>10,000	19 ± 5.3	53
2j	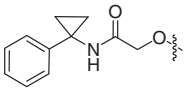		4.5 ± 0.8	12 ± 6.2	1.0 ± 0.4	>10,000	13 ± 0.5	46
2k	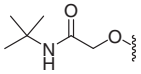		3413 ± 424	>10,000	ND	ND	1720 ± 178	ND
2l	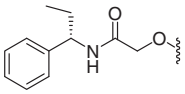		7.4 ± 0.5	20 ± 14	0.4 ± 0.01	1460 ± 572	8.6 ± 2.0	22
2m	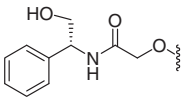		2.8 ± 0.5	6.7 ± 2.7	0.44 ± 0.01	1925 ± 807	6.1 ± 0.1	27
2n	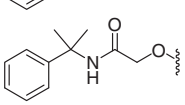		504 ± 14	ND	ND	>10,000	1370 ± 219	ND
2o	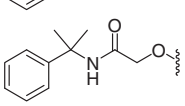		187 ± 2.6	ND	ND	>10,000	497 ± 227	83

(*continued on next page*)

Table 2 (*continued*)

Compd	R^1	R^3	CHO-hA_{2B} cAMP K_i (nM)	hA_{2B} binding K_i (nM)	HMC-1 IL-8 release K_i (nM)	Human A_{2A} binding K_i (nM)	A1 binding K_i (nM)	HLM stability (% remaining-0.5 h)
2p	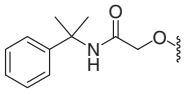		884 ± 12	ND	ND	>10,000	377 ± 29	ND
2q	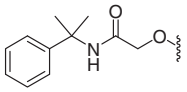		31 ± 2.0	ND	ND	2832 ± 27	12 ± 1	45

known SAR of the 8-phenyl xanthine analogs (such as MRS-1754). Interestingly, analog **1i** showed an increased stability in the HLM assay (64% remaining after 0.5 h) suggesting the *N*-benzyl amide was a metabolic liability. However, the importance of the *N*-benzyl group for potency was highlighted by the lack of activity in the *N*-cyclopropylmethyloxyacetamide **1j**. Additionally, a threefold drop in activity was noted in the *N*-methyl amide derivative **1k**. Overall, this initial study of the R^1 SAR did not result in an analog with higher A_{2B} binding affinity or increased activity in the A_{2B} cAMP functional assay. Furthermore, as is obvious from the data in Table 1, none of these derivatives addressed the issue of A_1 selectivity.

Attention was turned to the R^3 portion of the molecule (Table 2). While both a cyano group (**2a**) and furanyl group (**2b**) were tolerated at this position, inclusion of a 2-thiazolyl group at the R^3 position (**2c**) increased potency in the cAMP assay 17-fold (when compared to **1f**). Analog **2c** maintained good selectivity over the A_{2A} receptor (95-fold) but was still only threefold selective against the A_1 receptor. The human microsome stability of **2c** was also still poor.

Further investigation of the pendant 6-position side chain (R^1) was initiated while holding the more potent 3-(thiazol-2-yl)quinolinone scaffold constant. Derivatives of the 6-aminomethyl

Table 3
SAR of R^4 analogs

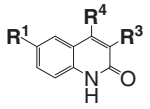

Compd	R^1	R^4	R^3	CHO-hA_{2B} cAMP K_i (nM)	Human A_{2B} binding K_i (mM)	HMC-1 IL-8 release K_i (μM)	Human A_{2A} binding K_i (mM)	A1 binding K_i (nM)	HLM stability (% remaining-0.5 h)
1a	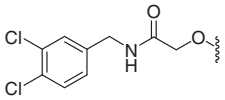	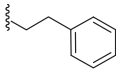		315 ± 102	211 ± 36	172 ± 106	>10,000	811 ± 6	0
3a	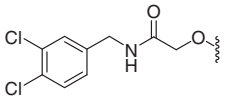			6670 ± 40	5251 ± 1389	1933 ± 694	>10,000	3914 ± 206	37
3b	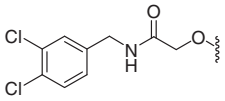			>10,000	ND	ND	>10,000	8603 ± 1757	0
2i	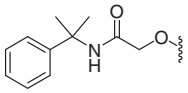	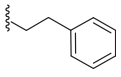		5.1 ± 1.1	28 ± 8.4	1.3 ± 0	>10,000	19 ± 5.4	53
3c	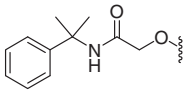			2669 ± 550	ND	ND	1080±524	5999 ± 1819	ND
3d	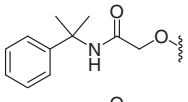	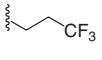		5155 ± 682	ND	ND	878±131	1129 ± 984	ND
3e	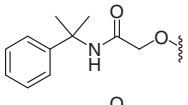	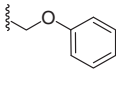		81 ± 6.7	70 ± 21	71 ± 37	>10,000	183 ± 101	12
3f	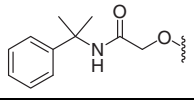	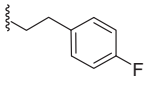		41 ± 0.2	105 ± 78	10 ± 0.2	>10,000	1153 ± 724	13

intermediate **18** (Scheme 3) were employed to test the requirement of the oxyacetamide group. While the 3-phenylpropanoyl derivative **2d** was only weakly active, the *N*-benzylurea analog **2e** was almost as potent as **1f**. This boost in potency when comparing analogs **2d** and **2e** suggests the nitrogen of the *N*-benzyl group may be acting as a hydrogen bond donor with the A_{2B} receptor. (This hypothesis is supported by the drop in potency exhibited by the N-methylated analog **1k** noted earlier.) An increase in the HLM stability of this urea series was achieved by the dimethylated benzyl analog **2f** (40% remaining after 0.5 h incubation).

The effect of substitution on the R^1 benzylic methylene of the lead structure **2c** was similarly investigated. The (*S*)-methyl-substituted analog (**2g**) maintained activity equal to the unsubstituted **2c** but the (*R*)-methyl-substituted analog **2h** was 15-fold less potent. Gratifyingly, the dimethyl-substituted derivative **2i** exhibited increased potency (5.1 nM) in the A_{2B} cAMP assay. As with analog **2f**, a significant increase in the microsomal stability was observed (53% remaining after 0.5 h incubation) for **2i**. The cyclopropyl analog **2j** was also a potent antagonist of the A_{2B} receptor with increased microsome stability, further implicating the benzylic methylene as a metabolic liability. The aromatic benzene ring proved again to be essential for the potency of these analogs since *t*-butyl amide **2k** was inactive. Both the ethyl- and hydroxyethyl-substituted analogs (**2l** and **2m**) were highly active in the A_{2B} related assays indicating that the boost in activity was not solely related to an increase in hydrophobicity in this area of the lead molecule.

The ability of these derivatives to suppress NECA-induced IL-8 release from HMC-1 cells was also examined (Table 2). This assay confirmed the results from the initial cAMP accumulation assay. Notably, analogs **2l** and **2m** inhibited the release of IL-8 at subnanomolar concentrations in this assay.

With the R^1 position optimized, attention returned to the R^3 heterocycle. The pyridine derivatives **2n**–**2p** were significantly less active than the benchmark compound **2i**. The 3-methyllisoxazole derivative, however, **2q** exhibited reasonable potency. Hence, it appears a five-membered heterocycle may be favored in this position.

The role of the 4-phenethyl group (R^4) was also investigated (Table 3). Replacement of the phenethyl group with a simple methyl group caused a >20-fold drop in A_{2B} binding affinity and cAMP activity (compare **1a** with **3a**). In addition, a 4-phenyl derivative (**3b**) was inactive. Furthermore, analogs bearing either a isobutyl- or 3,3,3-trifluoropropyl- group in the 4 position of the quinolinone (**3c** or **3d**) were significantly less potent then **2i**. Hence, the aromatic ring of the 3-phenethylgroup was an important contributor to the interaction of **2i** with the A_{2B} receptor.

A phenoxymethyl moiety (**3e**) could replace the phenethyl group albeit with a 15-fold drop in potency. *para*-Fluoro substitution of the phenethyl benzene (**3f**) also led to a moderate drop in A_{2B} activity but caused a modest increase in A_1 selectivity.

In summary, a series of 4-phenethylquinolinone A_{2B} antagonists was discovered. Optimization of the high throughput screening hits generated a lead molecule **2i** which was a potent (<10 nM) A_{2B} antagonist in in vitro functional assays. Significant improvements were made in the human liver microsome stability of these analogs. Future efforts will need to address the A_1 selectivity of this novel series.

References and notes

1. Jacobson, K. A. *Handbook of Experimental Pharmacology* **2009**, *193*, 1.
2. (a) Polosa, R. *Eur. Respir. J.* **2002**, *20*, 488; (b) Zhong, H.; Wu, Y.; Belardinelli, L.; Zend, D. *Am. J. Respir. Cell Mol. Biol.* **2006**, *35*, 587.
3. (a) Holgate, S. T. *Br. J. Pharmacol.* **2005**, *145*, 1009; (b) Kalla, R.; Zablocki, J. *Annu. Rep. Med. Chem.* **2009**, *44*, 265.
4. Ruesing, D.; Mueller, C. E.; Verspohl, E. J. *J. Pharm. Pharmacol.* **2006**, *58*, 1639.
5. Grant, M. B.; Davis, M. I.; Caballero, S.; Feoktistov, I.; Biaggioni, I.; Belardinelli, L. *Invest. Ophthalmol. Vis. Sci.* **2001**, *42*, 2068.
6. Eltzschig, H. K.; Jesus, R.-N.; Colgan, S. P. *Expert Opin. Ther. Targets* **2009**, *13*, 1267.
7. Fishman, P.; Bar-Yehuda, S.; Synowitz, M.; Powell, J. D.; Klotz, K. N.; Gessi, S.; Borea, P. A. *Handbook of Experimental Pharmacology* **2009**, *193*, 399.
8. Kim, Y.-C.; Ji, X.; Melman, N.; Linden, J.; Jacobson, K. A. *J. Med. Chem.* **2000**, *43*, 1165.
9. Elzein, E.; Kalla, R. V.; Li, X.; Perry, T.; Gimbel, A.; Zeng, D.; Lustig, D.; Leung, K.; Zablocki, J. *J. Med. Chem.* **2008**, *51*, 2267.
10. Vidal, B.; Nueda, A.; Esteve, C.; Teresa Domenech, T.; Benito, S.; Reinoso, R. F.; Pont, M.; Calbet, M.; López, R.; Cadavid, M. I.; Loza, M. I.; Cárdenas, Á.; Godessart, N.; Beleta, J.; Warrellow, G.; Ryder, H. *J. Med. Chem.* **2007**, *50*, 2732.
11. Eastwood, P.; Gonzalez, J.; Paredes, S.; Nueda, A.; Domenech, T.; Alberti, J.; Vidal, B. *Bioorg. Med. Chem. Lett.* **2010**, *20*, 1697.
12. Cheung, A. W.-H.; Brinkman, J.; Firooznia, F.; Flohr, A.; Grimsby, J.; Gubler, M. L.; Guertin, K.; Hamid, R.; Marcopulos, N.; Norcross, R. D.; Qi, L.; Ramsey, G.; Tan, J.; Wen, Y.; Sarabu, R. *Bioorg. Med. Chem. Lett.* **2010**, *20*, 4140.
13. Press, N. J.; Taylor, R. J.; Fullerton, J. D.; Tranter, P.; McCarthy, C.; Keller, T. H.; Brown, L.; Cheung, R.; Christie, J.; Haberthuer, S.; Hatto, J. D. I.; Keenan, M.; Mercer, M. K.; Press, N. E.; Sahri, H.; Tuffnell, A. R.; Tweed, M.; Fozard, J. R. *Bioorg. Med. Chem.* **2005**, *15*, 3081.
14. Cole, A. G.; Stauffer, T. M.; Rokosz, L. L.; Metzger, A.; Dillard, L. W.; Zeng, W.; Henderson, I. *Bioorg. Med. Chem. Lett.* **2009**, *19*, 378.
15. Shao, Y.; Cole, A. G.; Bresia, M.-R.; Qin, L.-Q.; Duo, J.; Stauffer, T. M.; Rokosz, L. L.; McGuinness, B. F.; Henderson, I. *Bioorg. Med. Chem. Lett.* **2009**, *19*, 1399.
16. McGuinness, B. F.; Cole, A. G.; Dong, G.; Brescia, M.-R.; Shao, Y.; Henderson, I.; Rokosz, L. L.; Stauffer, T. M.; Mannava, N.; Kimble, E. F.; Hicks, C.; White, N.; Wines, P. G.; Quadros, E. *Bioorg. Med. Chem. Lett.* **2010**, *20*, 6845.
17. (a) Ohlmeyer, M. H. J.; Swanson, R. N.; Dillard, L.; Reader, J. C.; Asouline, G.; Kobayishi, R.; Wigler, M.; Still, W. C. *Proc. Natl. Acad. Sci. U.S.A.* **1993**, *90*, 10922; (b) Burbaum, J. J.; Ohlmeyer, M. H. J.; Reader, J. C.; Henderson, I.; Dillard, L. W.; Li, G.; Randle, T. L.; Sigal, N. H.; Chelsky, D.; Baldwin, J. J. *Proc. Natl. Acad. Sci.* **1995**, *92*, 6027.
18. For details of the human liver microsome assay see: Merritt, J. R.; Liu, J.; Quadros, E.; Morris, M. L.; Liu, R.; Zhang, R.; Jacob, B.; Postelnek, J.; Hicks, C. M.; Chen, W.; Kimble, E. F.; Rogers, W. L.; O'Brien, L.; White, N.; Desai, H.; Bansal, S.; King, G.; Ohlmeyer, M. J.; Appell, K. C.; Webb, M. L. *J. Med. Chem.* **2009**, *52*, 1295.
19. *Representative spectral data*: For **2i**: ^{1}H NMR DMSO-d_6, 300 MHz: δ 8.23 (s, 1H), 8.13 (d, 1H), 7.92 (d, 1H), 7.39 (m, 5H), 7.29 (m, 4H), 7.20 (m, 3H), 4.69 (s, 2H), 3.55 (m, 2H), 2.95 (m, 2H), 1.56 (s, 6H). MS (ES-API): MH^+ = 524.2.
20. *hA_{2B} cAMP accumulation assay*: Chinese Hamster Ovary (CHO) cells (GlaxoSmithKline) stably transfected with the human A_{2B} receptor were maintained in 1× DMEM/F12 medium (Mediatech) supplemented with 10% FBS (Hyclone), 1% glutamax (Invitrogen), 0.1 U/ml adenosine deaminase (Roche Applied Science), 1% Penn/Strep (Invitrogen), 200 μg/ml G418 (Mediatech) and 200 μg/ml Hygromycin B (Mediatech). cAMP was quantified using the Perkin–Elmer LANCE™ cAMP 384 kit. On the day of the assay, 2500 CHO-hA_{2B} cells were pre-incubated with compound for 15 min and then stimulated with 75 nM NECA for 15 min in a final volume of 18 μL. Assay was conducted in 1× HBSS (Invitrogen), 5 mM HEPES (Invitrogen), 0.05% BSA, (Sigma), 100 μM papaverine–HCl (Sigma), pH 7.4 buffer at 37 °C/5% CO_2. Final DMSO concentration was 0.5%. Following stimulation, the cells were lysed with cAMP detection solution provided with the assay kit. Signal was allowed to develop for 1 h and detected using the EnVision™ Multiplate Reader or the Victor™ Multilabel counter (Perkin–Elmer Life and Analytical Sciences). Assays were performed in duplicate and compounds were tested a minimum of two times. The data were fit to a one-site competition binding model for IC_{50} determination using the program GraphPad Prism (GraphPad Software, Inc., San Diego, CA) and K_i values were calculated using the Cheng–Prusoff equation.
21. *hA_{2B} binding assay*: membranes (20 μg) prepared from CHO cells that stably express human A_{2B} (GlaxoSmithKline) were mixed with 30 nM (final) [^{3}H] ZM241385 in 50 μl assay buffer (50 mM Tris–HCl, pH 7.4, 100 mM NaCl, 10 mM $MgCl_2$, 1 mM EDTA, pH 6.5, 0.025 mg/ml adenosine deaminase (Roche Applied Science) containing 4% DMSO with or without test compounds. Reactions were carried out for 60 min at room temperature and were terminated by rapid filtration over GF/B filters (Millipore). Filters were washed four times with 1 ml cold 50 mM Tris–HCl, 100 mM NaCl, 10 mM $MgCl_2$, and radioactivity retained on filters was counted in a Microbeta Trilux microplate scintillation counter (Perkin–Elmer). Nonspecific binding was determined in the presence of 30 nM ZM241385. Assays were performed in duplicate and compounds were tested two times. Data were fit to a one-site competition binding model for IC_{50} determination using the program GraphPad Prism (GraphPad Software, Inc) and K_i values were calculated using the Cheng–Prusoff equation.
22. *HMC-1 IL-8 release assay*: HMC-1 human mast cells (Mayo Clinic Health Solutions) were maintained in IMDM (with 2 mM glutamine, Invitrogen), 10% iron-supplemented calf serum, 1% sodium bicarbonate (Invitrogen), 1% penicillin/streptomycin (Mediatech) and 1.2 mM α-thioglycerol (Sigma). On the day of the assay, compounds were prepared in growth medium containing 1 U/ml adenosine deaminase (Roche Applied Science) and 20 μM NECA (Sigma). To the compounds, 2.5×10^4 cells were added in 1:1 ratio to the prepared compounds/NECA (10 μM final concentration) in a final volume of 250 μL. Final DMSO concentration was 0.5%. Cells and compounds were incubated for 6 h at 37 °C/5% CO_2. Basal IL-8 release was determined in the

absence of NECA stimulation. Cell supernatant was collected and frozen at −80 °C until time of ELISA assay, when frozen supernatants were thawed and IL-8 release was quantified using the QuantiGlo Human IL-8 Chemiluminescent Immunoassay kit (cat no. Q8000B, R&D Systems). Chemiluminescent signal was captured using the Microbeta Trilux microplate counter (Perkin–Elmer Life and Analytical Sciences). Assays were performed in duplicate and compounds were tested two times. Data were fit to a one-site competition binding model for IC_{50} determination using the program GraphPad Prism (GraphPad Software, Inc., San Diego, CA) and K_i values were calculated using the Cheng–Prusoff equation.

23. For details on the A_{2A} and A_1 binding assays see the footnotes of Ref. 14. The values are reported as the mean of at least two determinations.
24. Like many adenosine receptor antagonists, these compounds generally exhibited poor aqueous solubility. Hence, the series with a lower *c* log *P* was favored.